Development of surface metrology for the Giant Magellan Telescope primary mirror

J. H. Burge[a,b], W. Davison[a], H. M. Martin[a], C. Zhao[b]

[a]Steward Observatory, University of Arizona, Tucson, AZ 85721, USA
[b]College of Optical Sciences, University of Arizona, Tucson, AZ 85721, USA

ABSTRACT

The Giant Magellan Telescope achieves 25 meter aperture and modest length using an *f*/0.7 primary mirror made from 8.4 meter diameter segments. The systems that will be used for measuring the aspheric optical surfaces of these mirrors are in the final phase of development. This paper discusses the overall metrology plan and shows details for the development of the principal test system – a system that uses mirrors and holograms to provide a null interferometric test of the surface. This system provides a full aperture interferometric measurement of the off-axis segments by compensating the 14.5 mm aspheric departure with a tilted 3.8-m diameter powered mirror, a 77 cm tilted mirror, and a computer generated hologram. The interferometric measurements are corroborated with a scanning slope measurement from a scanning pentaprism system and a direct measurement system based on a laser tracker.

Keywords: telescopes, optical fabrication, optical testing, aspheres

1. INTRODUCTION

The primary mirror for the Giant Magellan Telescope consists of a 25-m f/0.7 near-paraboloid made from a close packed array of seven 8.4-m segments.[1] This steep focal ratio provides for a short telescope, but it drives the aspheric departure to be quite large. The telescope and a plot of the 14.5-mm aspheric departure for one of the segments are shown in Figure 1. The fabrication of the first of these mirror segments, which is now underway, is covered in another paper.[2]

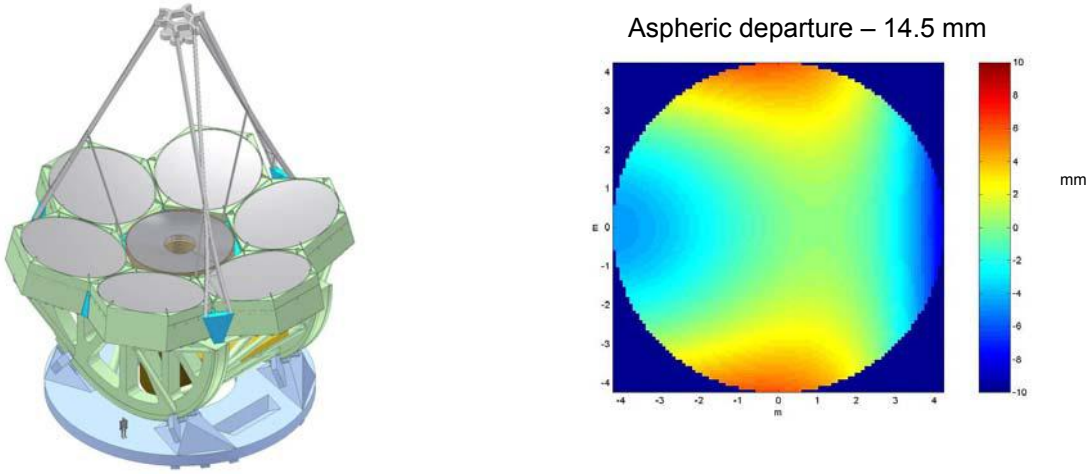

Figure 1. The 25-m *f* /0.7 GMT primary mirror is made of 8.4-m diameter segments. The off-axis segments have 14.5 mm departure from the best fitting sphere.

The designs and analysis for the metrology systems used to measure the aspheric surfaces were presented previously.[3,4] This paper discusses the production of the test hardware, being completed at the time of this writing. There are three different systems required to measure and confirm the shape of the GMT mirror segments:

jburge@optics.arizona.edu; phone 520-622-0170, fax 520-621-3389

Advanced Optical and Mechanical Technologies in Telescopes and Instrumentation, edited by Eli Atad-Ettedgui, Dietrich Lemke, Proc. of SPIE Vol. 7018, 701814, (2008) · 0277-786X/08/$18 · doi: 10.1117/12.790082

- Loose abrasive grinding is guided by measurements with a laser tracker system which is optimized for making these measurements with 1 μm rms accuracy. The concept and performance of this system are discussed here, and a separate paper discusses the details.[5]
- Full-aperture interferometric measurements will be used to guide the polishing and will provide the ultimate surface qualification. This system uses a vibration insensitive interferometer with HeNe source, a computer generated hologram, and two spherical reflectors 77 cm and 3.8-m in diameter. The production and alignment of this system provide the bulk of this paper.
- The final surface will be corroborated with a scanning pentaprism system that measures the surface slopes. The successful operation of a 1/5 scale prototype is covered in another paper.[6] The system being developed for GMT is presented below.

We present a comprehensive plan for measuring the GMT mirror segments that will allow us to have confidence that the optics will meet the stringent telescope requirements.

2. REQUIREMENTS FOR OPTICAL TESTING

The requirements for the optical measurements are derived from the telescope system specifications. These flow down as contributions to budgets for wavefront, support force, or geometric tolerances, as shown in Table 1. Fabrication errors in the primary mirror segments affect GMT in two ways: low order errors can be corrected but use some of the dynamic range of the active optics system, and the images are degraded by figure errors that are too small to correct. We have allocated a budget for optical testing errors that allows 25 N rms force per actuator for low order errors, out of an average force of 1070 N per actuator at zenith. The uncorrectable mirror surface figure errors due to measurement limitations are allocated a structure function 60% as large as the overall structure function specification for the surface.

Limited compensation in the telescope requires tight tolerances on off-axis distance, clocking angle (rotation of the segment about its mechanical axis), and matching radius of curvature among all seven segments. The segments' radii must be fabricated well enough in the lab that they can be adjusted in the telescope using the active support to give essentially a perfect match in the telescope. The departure from ideal will be compensated with the active optics. So the active optics allocation for the optical test must include the force required to correct a radius of curvature measurement error. This requires control of the 36 meter radius of curvature to accuracy of 0.3 mm.

Table 1. Error budget for GMT primary mirror segments, including allocation for optical test

Parameter	**Primary mirror**		**Optical Test**
	Specification	Goal	Allocation
Radius of curvature R	36,000.0 ± 1.0 mm	± 0.3 mm	± 0.3 mm
Conic constant k	-0.998286		
Clear aperture	8.365 m		
Off-axis distance	8710 ± 2 mm	± 1 mm	± 1 mm
Clocking angle	± 50 arcsec		± 50 arcsec
θ_{80} for structure function	0.166 arcsec	0.054 arcsec	<60% of SF for 0.166 arcsec
Scattering loss L at λ = 500 nm	< 2.0%	< 1.5%	
Actuator correction forces	< 50 N rms		<25 N rms

We have imposed an additional requirement for the program – that redundant optical measurements are required for each important parameter. We have developed an independent measurement for large scale mirror surface and slope errors, as well as a method of calibrating small scale test errors and for fine sampling the edge.

3. INITIAL METROLOGY WITH LASER TRACKER PLUS

During early stages of fabrication, the optical surface is measured using a commercial laser tracker mounted above the mirror in the test tower. The laser tracker is a three-dimensional coordinate measurement system that directs a laser beam toward a retroreflector and uses the gimbal angles (from encoders) and radial distance (from distance measuring interferometry or DMI) to determine its position. To measure the optical surface we move an SMR (sphere-mounted retroreflector) across the surface and use the DMI to measure the relative change in distance. This system, shown in Figure 2, has two important features:

- It does not require a specular surface, so we can use this system to measure the rough surface to guide the generating and loose abrasive grinding operations.
- We can measure low order shape errors in the polished surface to < 1 μm by augmenting the laser tracker with additional references, calibrating the tracker errors, and measuring multiple points across the mirror to reduce the effects of noise. This provides an independent corroboration of the mirror shape.

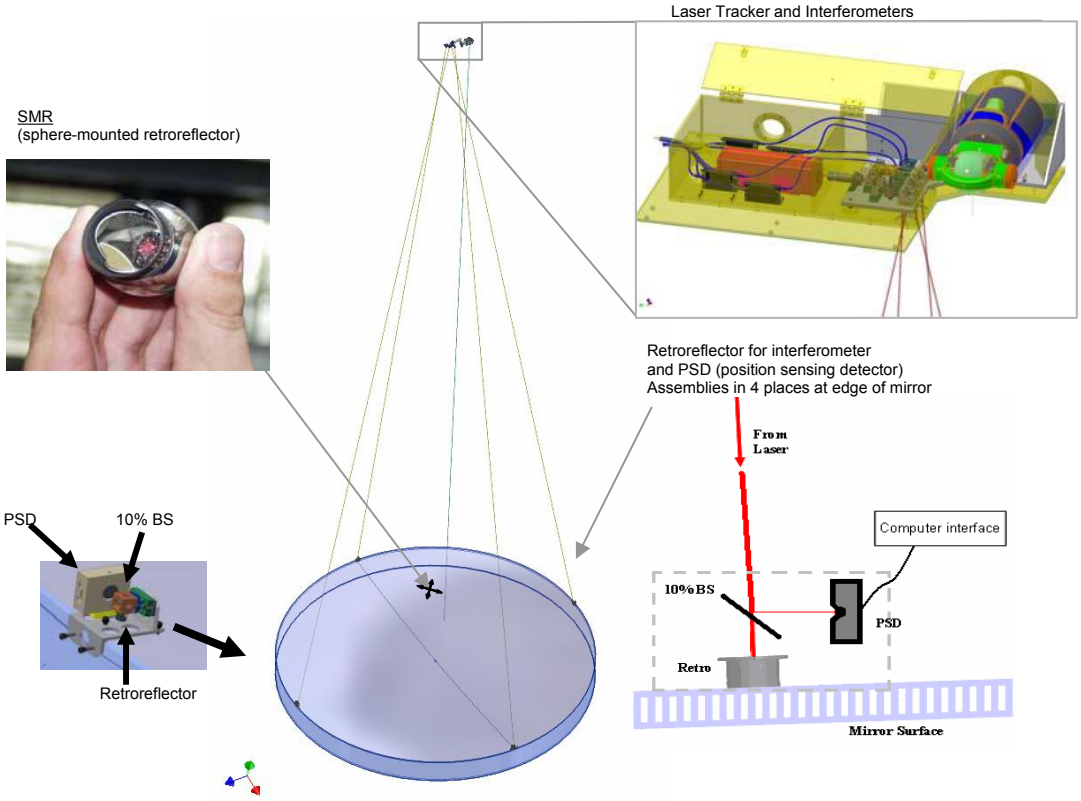

Figure 2. Configuration of the laser tracker set up for measuring the mirror surface. The laser tracker uses interferometry to measure distance to an SMR (sphere-mounted retroreflector). The tracker runs under servo control to follow the ball as it is scanned across the surface, combining radial distance with the gimbal angles to make a three-dimensional measurement. Effects due to the combined motion of the air, mirror, and tracker are mitigated by separate real-time measurements of distance and lateral motion using four interferometer/position sensing detector systems.

The system, which we call *Laser Tracker Plus,* has been completed and mounted into the test tower at the Steward Observatory Mirror Lab. The system consists of the laser tracker plus stability references and *in situ* calibration of radial and angular errors. Preliminary measurements of indicate that this system is capable of measuring the GMT mirror to < 1 μm rms. Details of this system are presented in another paper in these proceedings.[5]

4. PRINCIPAL SURFACE MEASUREMENTS WITH INTERFEROMETRY

The principal optical test is a full-aperture, high-resolution measurement of the figure, made by phase-shifting interferometry with a null corrector to compensate for the aspheric surface. The null corrector compensates for 14 mm of aspheric departure in the off-axis segment, as shown in Figure 1. The accuracy of the principal test is specified so that low order aberrations from errors in the test can be corrected in the telescope using a combination of budgeted small displacements of the segment and bending with the active supports.

4.1 System design and alignment

Figure 3 shows the layout of the principal interferometric test. The null corrector uses two spherical mirrors and a computer-generated hologram to transform the interferometer's spherical wavefront into a test wavefront that matches the surface of the segment. Most of the compensation is made by an oblique reflection off a 3.75 m spherical mirror (M1). A similar reflection off a 77 cm diameter spherical mirror (M2) makes further compensation, and the hologram is designed to eliminate the residual error.

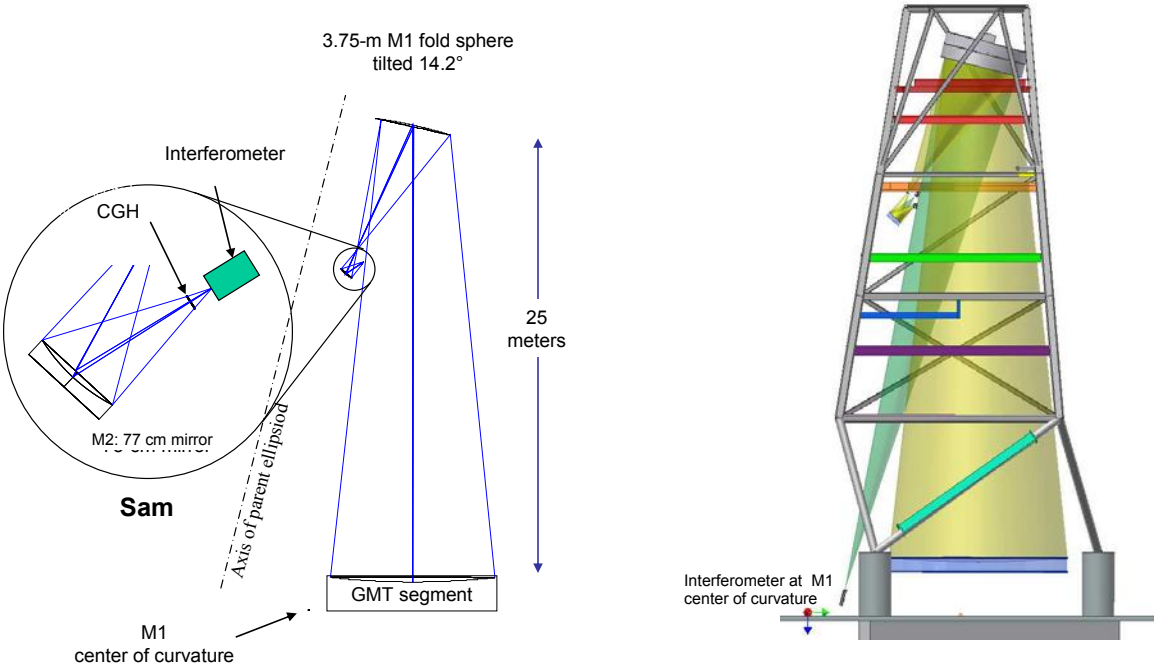

Figure 3. Optical layout for the interferometric measurements of the off axis GMT mirror segments. The optical diagram and the layout in the Steward Observatory Mirror Lab test tower are shown.

The parameters for the two mirrors in the system are listed in Table 2. Figure errors in the 3.75-m diameter fold sphere M1 would cause significant errors in the GMT test, so M1 will be measured from its center of curvature simultaneously with the measurement of the GMT segment and its errors will be subtracted from the GMT measurement. The smaller M2 will be made to tight tolerances.

Figure 4 and Figure 5 show the small optical assembly including the interferometer, hologram and M2. We call this small optical assembly "Sam" for short. Sam also includes critical mechanical components and alignment tools, as well as a reference hologram that is inserted into the system for calibration and alignment. Achieving such a large compensation is challenging and requires great attention to the alignment of all parts of the test.

Table 2. Some parameters of the test geometry. The central ray is the ray that hits the mechanical center of the GMT segment.

parameter	value
3.75 m sphere (M1)	
radius of curvature	25.5 m
distance from GMT segment	23.5 m
angle of incidence, central ray	14.2°
0.77 m sphere (M2)	
radius of curvature	1.37 m
distance from 3.75 m sphere	8.3 m
angle of incidence, central ray	14.5°

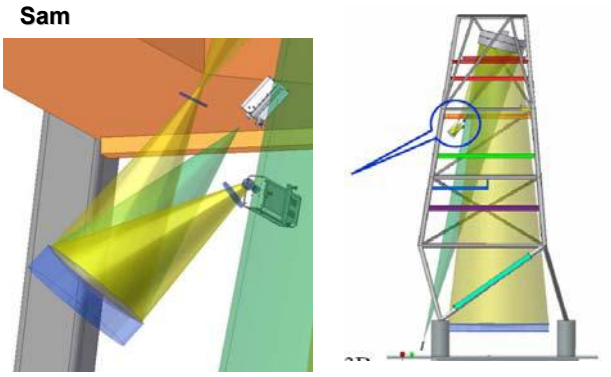

Figure 4. Small optical assembly (Sam) for the GMT principal test

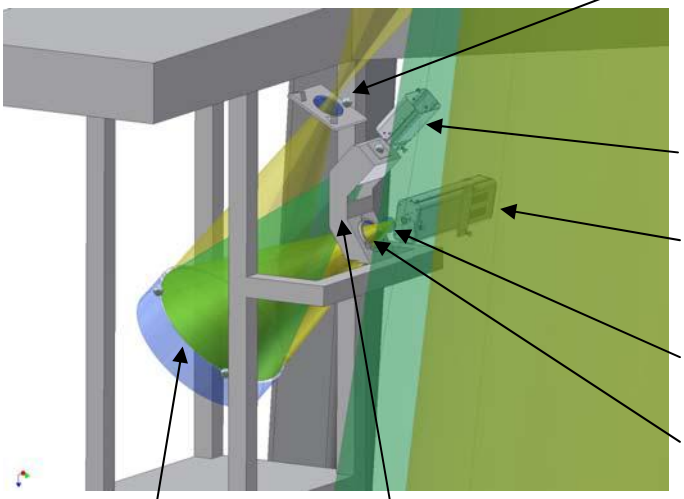

Figure 5. Optical components for the small optical assembly (Sam) for the GMT principal test. In invar reference (the cradle) maintains the position reference between the CGH and M2. A reference hologram can be inserted to calibrate the wavefront from Sam.

The components of Sam are mounted in a steel frame attached to the third platform of the test tower. Critical dimensions are maintained by a small invar frame (the cradle) that supports the measurement hologram and a ball at the center of curvature of M2 (the M2 CoC ball), and by three invar metering rods that constrain M2 relative to the cradle in piston, tip and tilt. The cradle is mounted kinematically in the steel frame, with no adjustments. The M2 ball and the hologram are separated by only 440 mm, so the cradle can be relatively small.

Figure 6. The invar cradle is used to provide the reference for the most critical dimensions in the optical test. The position of M2 is adjusted so that its center of curvature coincides with the M2 reference ball, which is attached to the cradle. The position of this reference ball, with respect to the CGH is controlled to < 10 µm over the distance of 44 cm.

The measurement hologram is the fixed component in the system. Within Sam, the two optical components that must be aligned to the hologram are the interferometer and M2. The most challenging task is aligning M2 to the hologram, and keeping it aligned, to an accuracy of about 20 µm in three degrees of freedom. The hologram, shown in Figure 7, is written on a 15 cm square, 6 mm thick glass substrate. We bond mounting and reference features onto the glass surface, and use an optical CCM to locate the references to about 5 µm accuracy. We mount the hologram semi- kinematically on the cradle using a flexure to connect two of the mounting balls without overconstraint. The cradle also contains a kinematic mount for the M2 CoC ball. The ball's mount is adjusted by shims based on CMM measurements with respect to the CGH references to provide an accurate reference.

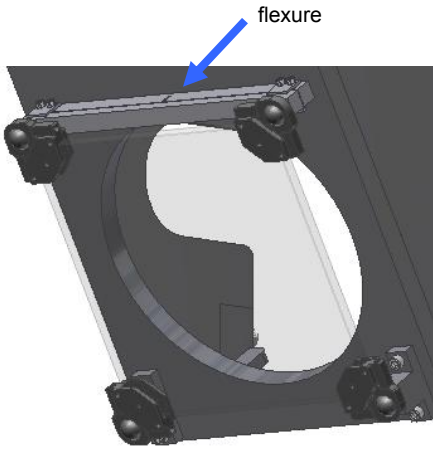

Figure 7. The 15 x 15 cm CGH is supported semi-kinematically from attachments at the four corners.

Having maintained accuracy for the M2 reference ball, we align M2 using a Point Source Microscope (PSM), as shown in Figure 8. We first align the PSM to the reference ball, then we remove the reference ball, allowing the PSM to see M2. The tip, tilt, and axial shift for M2 are then adjusted by three actuators connected to invar metering rods (Figure 9) until the reflecting light matches the reflection that was measured from the reference ball.

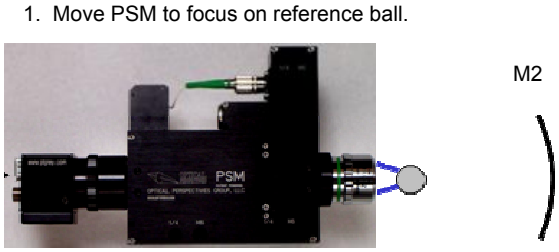

Figure 8. The Point Source Microscope is used as feedback to move M2 to place its center of curvature to coincide with the reference ball position.

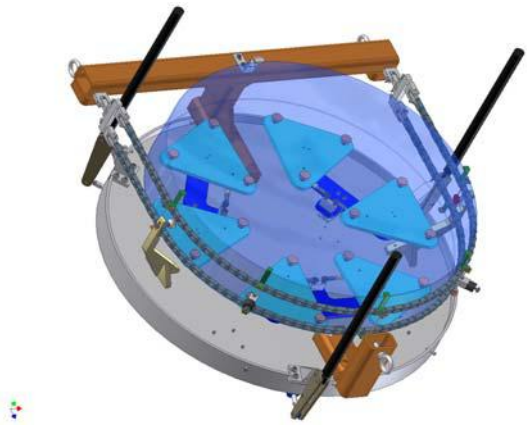

Figure 9. The 77-cm M2 is mounted using a conventional whiffle tree type support. The position is maintained with three invar rods that attach to the support cell.

We align the interferometer to the measurement hologram by viewing a pattern written on the hologram that returns a spherical wavefront back to the interferometer as shown in Figure 10. For control of tilt, we use reflection from an annular CGH pattern surrounding the main test pattern (the pattern that forms part of the null corrector). The annular pattern and the possible substrate distortion give poor resolution for focus measurement from this pattern. We use a third pattern for this purpose which uses the region in the corners of the substrate. This pattern produces collimated light in transmission for the correct focus. We measure this by inserting an autocollimating flat mirror and setting the interferometer axial position based on the return fringes to provide a null.

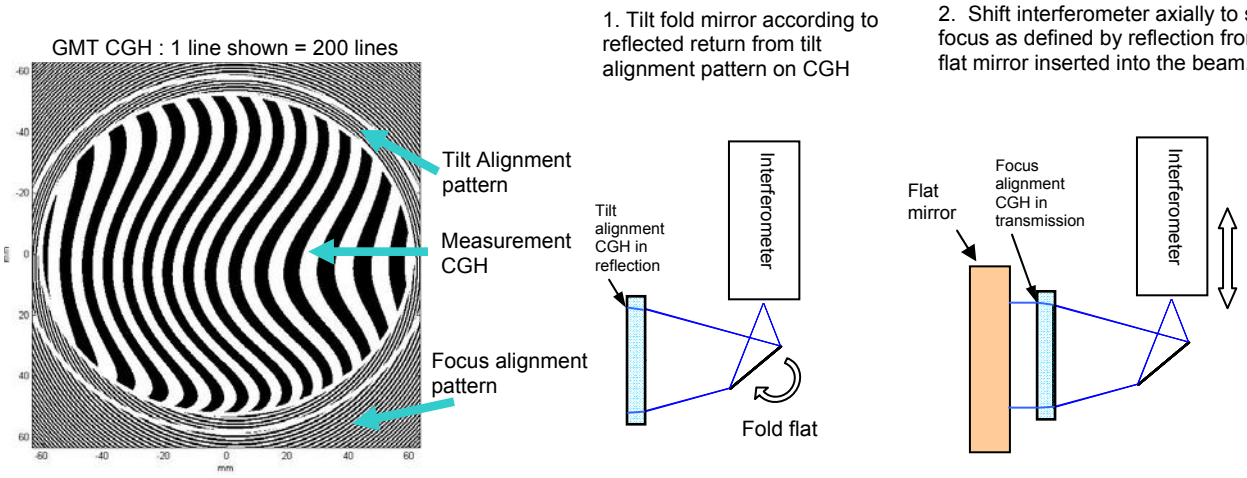

Figure 10. The interferometer is aligned to the CGH according to measurements from two alignment patterns. Light from the tilt alignment pattern is reflected into the interferometer and gives feedback for the substrate tilt with respect to the spherical interferometer beam. The focus alignment pattern nominally collimates the light. This is measured using a flat mirror in autoreflection. The interferometer focus is moved axially based on this measurement.

A second CGH, the reference hologram, is inserted near Sam's internal focus to measure the wavefront from Sam and to provide accurate references for aligning Sam to the larger mirrors. The reference hologram, shown in Figure 11, reflects the wavefront back into Sam to calibrate it in the same way we calibrate other null correctors.[7] The reference hologram becomes an essential part of the alignment of the rest of the optical system—M1 and the GMT segment—relative to Sam. The reference hologram is semi-kinematically mounted on an invar plate that also holds the references used in the system alignment. The reference hologram is aligned to Sam's wavefront to return a null wavefront to the interferometer. Once it is in that position, its alignment references are measured with a laser tracker to determine the position of Sam's *outgoing wavefront*. This measurement must be available on demand, so remotely controlled actuators are used to insert, align, and retract the reference hologram.

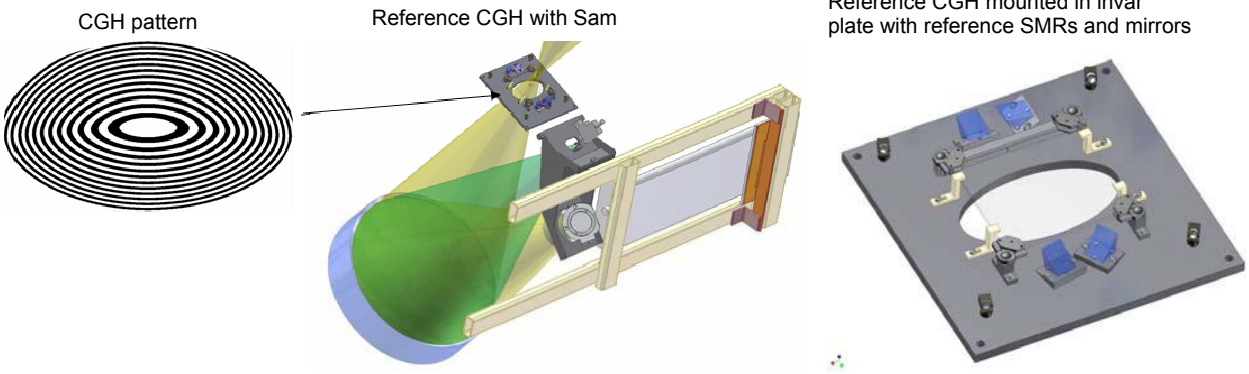

Figure 11. The reference hologram is inserted into Sam's outgoing wavefront to check the performance of Sam and to provide references that are used for a laser tracker to determine Sam's position. The reference CGH is mounted to an invar plate. Tracker reference balls and mirrors are aligned to the CGH and bonded to the plate.

The relative alignment between Sam, the 3.75-m fold sphere, and the GMT mirror segment are measured using a dedicated laser tracker that is mounted in the test tower. The location of Sam is fixed in the tower and its position is determined by measuring the location of the reference CGH when it is adjusted to match the wavefront from Sam. The large fold sphere M1 is measured using a combination of SMRs on the surface and an SMR at its center of curvature. The M1 cell is supported on actuators that are adjusted to place the mirror in the correct place with respect to Sam as measured by the laser tracker. The location of the GMT segment then is measured using SMRs on the surface. Support actuators on the GMT segment are then adjusted to place it in the correct location with respect to the optical test.

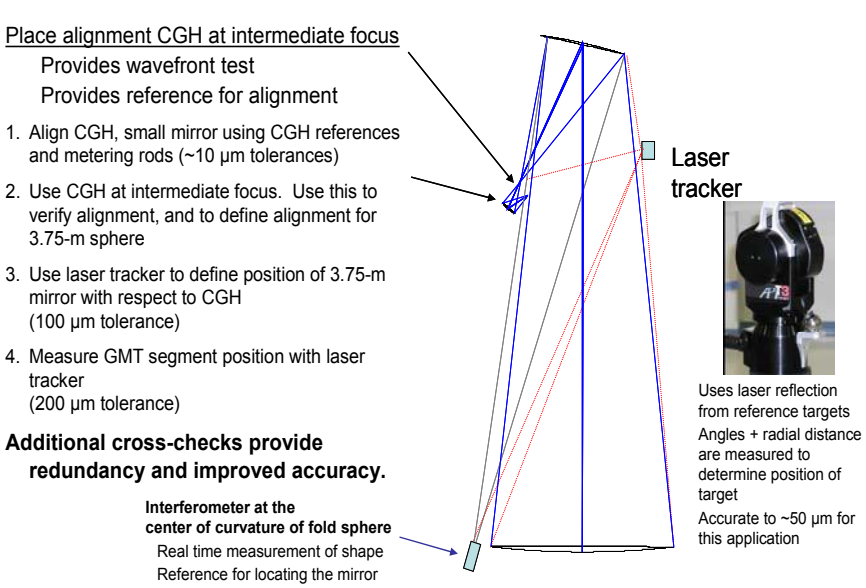

Figure 12. The position of Sam, the 3.75-m fold sphere M1, and the GMT segment are measured using a laser tracker. M1 and the GMT segment are moved with actuators according to the laser tracker data.

The position of the reference CGH is measured using SMRs that are attached to the CGH mounting plate as shown in Figure 11. The positions of these references are measured with respect to the optical pattern on the CGH using an optical CMM. The accuracy of the tracker is not sufficient to determine the orientation of the CGH directly. We bond mirrors to the CGH mounting plate and measure the angle with respect to the CGH. Then the orientation of a mirror normal is determined by the laser tracker by comparing the true position of an SMR with the apparent position created by a reflection. A complete analysis of this method is given in another paper.[8] The geometry for this measurement is shown in Figure 13.

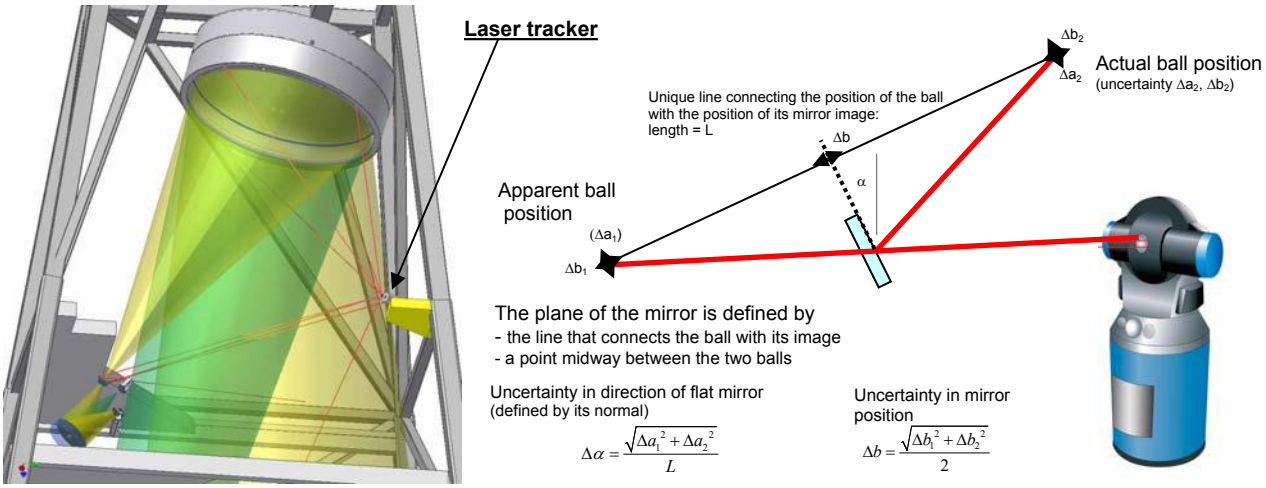

Figure 13. The laser tracker in the tower is used to measure the position of M1, Sam's reference CGH, and the GMT mirror (not shown). The orientation of the reference CGH is measured using mirrors that are co-aligned to the CGH. The tracker determines the mirror normal direction as the line that connects the mirror image of an SMR with the actual SMR position.

4.2 Error analysis for principal interferometric test

The analysis of the optical test was performed in terms of the effects that such errors may have on GMT performance. We carefully track the impact of component or subsystem errors on the resulting mirror geometry, the forces required to correct controllable modes, and the residual uncorrectable error. The analysis assumes optimal compensation using the rigid body motion of the mirror segments to minimize the force required for bending.[3] The effect of figure errors that cannot be corrected with active optics is quantified in terms of a wavefront structure function. We compare this directly with the GMT requirement for the mirror itself.

We treat two different types of errors, alignment errors due to position errors and low order distortion, and figure errors in the components. The effect of alignment errors is determined by direct simulation and the effect of figure errors is taken as a direct calculation.

4.2.1 Accuracy of holograms

The measurement hologram is used in transmission, so surface errors or refractive index variations in the glass will cause errors in the diffracted wavefront, primarily on large scales. These errors, along with errors in the interferometer and fold flat, will be measured with the wavefront calibration mirror and removed from the data. We can achieve accuracy of better than 5 nm rms in the surface of the GMT segment.

Distortion in the fringe pattern, which can come from manufacturing limitations, will cause an error in the wavefront. The coupling of pattern distortion to wavefront error depends on the line spacing. The measurement hologram has a nominal line spacing of about 20 μm. We will have it fabricated using electron beam lithography, which is accurate to 0.1 μm. (The standard quality-control check for e-beam patterns includes a measurement to prove that the pattern is accurate to 0.1 μm.) Pattern distortion of 0.1 μm will cause λ/200 wavefront error for each pass through the hologram, so the test accuracy for the GMT surface will be degraded by 3 nm rms. While we do not have a way to verify independently the wavefront accuracy of the hologram for the GMT test, we will have one or more holograms made that

have similar specifications (such as size and line spacing) but convert a spherical wavefront to a different spherical wavefront that can be measured directly. We have used this practice for several aspheric holograms in the past and confirmed the accuracy of the process.

The reference hologram uses 3rd-order diffraction and has a nominal line spacing of 4 μm, so the errors due to 0.1 μm pattern distortion will be about 50 nm of wavefront. This does not affect the GMT measurement directly, only the alignment of M1. Substrate distortion has a larger, but still insignificant, effect on the alignment of M1, and it is included in

4.2.2 M2 figure

The specification for M2 is a structure function of the same form as that for the GMT segment. The amplitude of M2's specification is set so that the error due to M2 in double pass is less than 20% of the GMT specification. A spatial scale of 9 mm on M2 corresponds to about 100 mm on the GMT segment, and this is the smallest scale on which we would actively figure the segment. We are less concerned about errors in M2 on smaller scales; they only make the GMT segment *look* worse than it really is. The structure function specification for M2 allows rms surface errors ranging from 6 nm on a scale of 100 mm to 1.3 nm on a scale of 10 mm. In addition, up to 70 nm rms surface astigmatism is allowed. These errors are allocated equally between fabrication and support on larger scales, while most of the error is allocated to fabrication on small scales. We have analyzed an 18 point whiffletree support and found that it comfortably meets the support requirements.

4.2.3 M1 figure

We will measure the figure of M1, shown in Figure 14, as part of each measurement of the GMT segment, and compensate for its figure error. The accuracy of the GMT measurement depends on the accuracy of this compensation. In order to avoid adding noise to the GMT measurement, we will smooth the measurement of M1 to a resolution of around 100 mm, and use this low-resolution map as a reference that is subtracted from the map of the GMT segment. To make this subtraction we must correct for mapping between the images of M1 in the two measurements. An error in mapping causes us to subtract the right figure error from the wrong location on the GMT segment.

Figure 14. The 3.75 m fold sphere (M1) on the polishing machine (left) and after coating (right).

The error in subtracting the reference is equal to the scalar product of the slope error in the reference map and the mapping error. This will probably be the dominant error in the measurement of the GMT segment on scales of 100-1000 mm. The dominant error on smaller scales will probably be due to structure on M1 that is not represented in the smoothed reference map. The precise resolution of the reference map will be set to minimize the net error and will depend on the small-scale accuracy of the *in situ* measurement of M1. More smoothing of the reference map decreases its slope errors but increases the uncorrected small-scale structure.

M1 has been finished to an accuracy of better than 20 nm rms surface over its clear aperture. We expect an accuracy of about 15 nm rms after optimizing support forces when M1 is mounted in the tower. The figure meets the requirements for slope error in the smoothed reference map (< 2 nm/cm rms surface slope) and small-scale error in the residual high-frequency map (<15% of the GMT segment specification). An additional requirement for the *in situ* measurement is an rms mapping error < 1.5 cm.

4.2.4 Alignment accuracy

The effects from misalignment were determined by direct simulation. Each component has multiple sources of alignment error. We have assumed tolerances corresponding to ±2 σ for individual contributions and combined them in root sum square to estimate the resulting uncertainty. The effect on the system performance is then determined by direct simulation. A summary of the alignment errors for this test is given in Table 3.

Table 3. Effects of uncertainty showing the contribution of each component of misalignment to the shifts in off-axis distance and clocking angle, correction force, and residual surface error. Displacements are in μm, tilts in μrad, and astigmatism in nm rms surface. Coordinates *x*, *y* and *z* are local to each component with the *z* axis perpendicular to the surface and the *y* axis intersecting the parent optical axis.

element	parameter	uncertainty (μm, μrad)	Effect on GMT mirror segment			
			radial shift (mm)	clocking (arcsec)	correction force (N rms)	residual rms surface (nm)
interferometer	*X*	2	0.0	0	0.2	0.2
	Y	2	0.0	0	0.6	0.6
	Z	11	0.0	0	2.3	2.7
M2	*x*	22	0.0	0	1.4	1.5
	y	22	0.0	0	4.6	5.2
	z	13	0.0	0	2.0	1.8
	R	20	0.0	0	0.4	0.4
	0° astig	50 nm	0.0	0	1.0	1.0
	45° astig	50 nm	0.0	0	0.7	0.5
reference hologram	*x*	61	0.0	0	0.3	0.5
	y	62	0.2	0	1.2	1.5
	z	61	0.6	0	3.5	4.9
	θ_x	21	0.0	0	4.3	4.3
	θ_y	22	0.0	1	1.6	1.6
	θ_z	31	0.0	2	0.8	0.8
M1	z	73	0.8	0	6.0	8.0
	θ_x	7.7	0.4	0	3.0	3.0
	θ_y	7.7	0.0	4	0.9	0.9
	R	200	0.3	0	1.3	1.9
	0° astig	100 nm	0.0	0	1.6	2.1
	45° astig	100 nm	0.0	3	1.1	1.3
GMT segment	*z*	120	0.2	0	2.7	3.2
components of Sam, not measured with reference hologram			0.2	3	7.1	7.4
Sum in quadrature			1.2	6	13.4	15.4

The structure function from both alignment and figure effects are added and shown to fit well within the requirements for the optical test.

5. CORROBORATING MEASUREMENTS OF THE GMT SURFACE

We are implementing two additional tests of the GMT segments to verify the final accuracy:

- A scanning pentaprism test measures the low order shape errors. This test is presented in another paper in this conference.[6]
- A shear test (the GMT segment is moved under the test system) measures small scale errors. This has been presented in other papers.[4, 9]

The set of tests that we are building for GMT has been difficult and expensive to develop. But this equipment allows rapid fabrication of all of the mirror segments, which will enable the telescope to be built at moderate cost and very low risk.

Optical Test	**Function**	**Purpose**	**Performance**
Principal test Interferometry using fold spheres + CGH	Measure entire surface to ~2 cm spatial resolution	Guide polishing, qualify finished surface	Low order: correctable with <25 N rms actuator force Higher order: <30 nm rms surface irregularity
Scanning pentaprism measurements	Measure surface errors corresponding to lowest bending modes	Redundant test for low order shape, including RoC	Lowest order modes: correctable with <20 N rms actuator force
Laser Tracker (plus references)	Measure surface with ~60 cm spatial resolution	Guide coarse figuring Redundant test of shape	~1 μm rms 0.25 μm rms goal
Shear test using principal interferometric test	Shift mirror to allow separation of test errors from mirror features	Redundant test of high order figure errors	< 20 nm rms

6. REFERENCES

1) M. Johns, "The Giant Magellan Telescope (GMT)", in *Ground-based and Airborne Telescopes*, ed. L. M. Stepp, Proc. SPIE 6267 (2006).
2) H. M. Martin, J. H. Burge, B. Cuerden, W. B. Davison, J. S. Kingsley, W. C. Kittrell, R. D. Lutz, S. M. Miller, C. Zhao and T. Zobrist, Progress in manufacturing the first 8.4 m off-axis segment for the Giant Magellan Telescope in *Advanced Optical and Mechanical Technologies in Telescopes and Instrumentation*, ed. E. Atad-Ettedgui and D. Lemke, Proc. SPIE **7018** (2008; these proceedings).
3) J. H. Burge, L. B. Kot, H. M. Martin, R. Zehnder, C. Zhao, "Design and analysis for interferometric measurements of the GMT primary mirror segments", in *Optomechanical Technologies for Astronomy*, ed. E. Atad-Ettedgui, J. Antebi and D. Lemke, Proc. SPIE 6273 (2006).
4) J. H. Burge, L. B. Kot, H. M. Martin, C. Zhao, T. Zobrist, "Alternate surface measurements for GMT primary mirror segments", in *Optomechanical Technologies for Astronomy*, ed. E. Atad-Ettedgui, J. Antebi and D. Lemke, Proc. SPIE 6273 (2006).
5) T. Zobrist, J. H. Burge, W. Davison and H. M. Martin, "Measurement of large optical surfaces with a laser tracker", in *Advanced Optical and Mechanical Technologies in Telescopes and Instrumentation*, ed. E. Atad-Ettedgui and D. Lemke, Proc. SPIE 7018 (2008; these proceedings)..
6) P. Su, J. H. Burge, B. Cuerden and H. M. Martin, "Scanning pentaprism measurements of off-axis aspherics", in *Advanced Optical and Mechanical Technologies in Telescopes and Instrumentation*, ed. E. Atad-Ettedgui and D. Lemke, Proc. SPIE 7018 (2008; these proceedings).
7) J. H. Burge, "Certification of null correctors for primary mirrors," in *Advanced Optical Manufacturing and Testing IV*, J. Doherty, Editor, Proc. SPIE **1994**, 248-259 (1993)
8) J. H. Burge, P. Su, T. Zobrist, C. Zhao, "Use of a commercial laser tracker for optical alignment" in *Optical System Alignment and Tolerancing*, ed. by J. Sasian and M. Ruda, Proc. SPIE **6676**, (2007).
9) P. Su, J. Sasian, and J. H. Burge, "Shear test of off-axis surface with axi-symmetric parent," in *Optical Manufacturing and Testing VII*, ed. by J. Burge, O. Faehnle, and R. Williamson, Proc. SPIE **6671**, (2007).